MIT Open Access Articles

*Study of CP violation in B[superscript #] →
D[superscript #] (h =K,π) with the modes D →
K[superscript #]π[superscript ±]π[superscript 0], D
→ π[superscript +]π[superscript -]π[superscript 0]
and K[superscript +]K[superscript -]π[superscript 0]*

Study of *CP* violation in $B^{\mp} \to Dh^{\mp}$ ($h = K, \pi$) with the modes $D \to K^{\mp}\pi^{\pm}\pi^0$, $D \to \pi^+\pi^-\pi^0$ and $D \to K^+K^-\pi^0$

R. Aaij *et al.*[*]

(LHCb Collaboration)

An analysis of the decays of $B^{\mp} \to DK^{\mp}$ and $B^{\mp} \to D\pi^{\mp}$ is presented in which the D meson is reconstructed in the three-body final states $K^{\mp}\pi^{\pm}\pi^0$, $\pi^+\pi^-\pi^0$ and $K^+K^-\pi^0$. Using data from LHCb corresponding to an integrated luminosity of 3.0 fb^{-1} of pp collisions, measurements of several *CP* observables are performed. First observations are obtained of the suppressed Atwood-Dunietz-Soni decay $B^{\mp} \to [\pi^{\mp}K^{\pm}\pi^0]_D\pi^{\mp}$ and the quasi-Gronau-London-Wyler decay $B^{\mp} \to [K^+K^-\pi^0]_D\pi^{\mp}$. The results are interpreted in the context of the unitarity triangle angle γ and related parameters.

I. INTRODUCTION

Precise measurements of the parameters of the Cabibbo-Kobayashi-Maskawa unitarity triangle [1] are of great value in searching for manifestations of new physics in the flavor sector. In particular, the determination of the angle $\gamma \equiv \arg(-V_{ud}V_{ub}^*/V_{cd}V_{cb}^*)$ (also denoted as ϕ_3 in the literature) in processes involving tree-level decays provides a Standard Model benchmark against which observables more sensitive to new physics contributions can be compared. Currently such comparisons are limited by the uncertainty on γ, which is $\sim 7°$ [2–5]. More precise measurements and new analysis strategies are, therefore, required.

Sensitivity to γ in tree-level processes may be obtained through the study of *CP*-violating observables in the decays $B^{\mp} \to Dh^{\mp}$, where D indicates a neutral charm meson which decays in a mode common to both D^0 and $\bar{D}^0$ states, and h, the bachelor hadron, is either a kaon or a pion. In the case of $B^- \to DK^-$, interference occurs between the suppressed $b \to u\bar{c}s$ and favored $b \to c\bar{u}s$ quark-level transitions and, similarly, for the charge-conjugate decay. The magnitude of the interference is governed by three parameters: the weak-phase difference, γ, the *CP*-conserving strong-phase difference, δ_B, and the ratio of the magnitudes of the two amplitudes, r_B. Similar interference effects occur in the case when the bachelor hadron is a pion, but then additional Cabibbo suppression factors mean that the sensitivity to γ is much reduced. Many classes of D decay can be exploited. Important examples include the so-called Atwood-Dunietz-Soni (ADS) modes [6], which are decays to quasiflavor

eigenstates such as $D \to K^{\mp}\pi^{\pm}$, and the Gronau-London-Wyler (GLW) modes [7], which are decays to *CP* eigenstates such as $D \to K^+K^-$. Measurements exist from LHCb that follow both the ADS and GLW approaches [8–11], as well as alternative methods [12,13].

In the case that the D meson decays to three or more hadrons, the interference effects that are sensitive to γ vary over the phase space of the D decay due to the role of strongly decaying intermediate resonances. If the D decay is analyzed inclusively, the integration over phase space in general dilutes the net sensitivity. For multibody ADS modes the dilution factor can be measured with $D\bar{D}$ pairs coherently produced at the $\psi(3770)$ resonance [14]. LHCb has previously made use of such measurements performed with data from the CLEO-c experiment [15–17] in $B^{\pm} \to Dh^{\pm}$ analyses exploiting the modes $D \to K^{\mp}\pi^{\pm}\pi^-\pi^+$ [9] and $D \to K_S^0 K^{\mp}\pi^{\pm}$ [10]. It has recently been pointed out [18] that similar considerations apply to self-conjugate multibody modes such as $D \to \pi^+\pi^-\pi^0$. These modes approximate to *CP* eigenstates and, hence, a $B^{\mp} \to DK^{\mp}$ analysis that employs them can be considered a quasi-GLW (qGLW) analysis. In this case the dilution factor is related to how closely the mode approaches a *CP* eigenstate, and can also be measured at the open charm threshold.

This paper presents the measurement of *CP* observables from $B^{\pm} \to Dh^{\pm}$ decays, where D mesons are reconstructed using three different multibody final states. These decays are the ADS channel $D \to K^{\mp}\pi^{\pm}\pi^0$ and the qGLW modes $D \to \pi^+\pi^-\pi^0$ and $D \to K^+K^-\pi^0$. In all cases, higher sensitivity is attained compared with the results of the previous measurements which exist from the *BABAR* [19] and Belle [20] Collaborations for the ADS channel, and from *BABAR* for the mode $D \to \pi^+\pi^-\pi^0$ [21]. Measurements at the $\psi(3770)$ resonance [15,16,18] indicate that the dilution effects in $D \to K^{\mp}\pi^{\pm}\pi^0$ and $D \to \pi^+\pi^-\pi^0$ are rather small, making these decays particularly suitable for an inclusive analysis.

---

[*]Full author list given at the end of the article.

This paper is organized as follows. Section II introduces the observables that the analysis seeks to measure, and explains how they are related to the underlying physics parameters and the dilution factors that are determined externally. Section III describes the LHCb detector and the data set on which the analysis is based. Sections IV and V present the candidate selection and the analysis procedure. Results are given in Sec. VI, together with a discussion of the systematic uncertainties. In Sec. VII the measured observables are interpreted in terms of γ and the other physics parameters, and conclusions are drawn.

II. OBSERVABLES AND EXTERNAL INPUTS

In the ADS channel there exist two suppressed modes, $B^{\mp} \to [\pi^{\mp}K^{\pm}\pi^0]_D h^{\mp}$, and two favored modes, $B^{\mp} \to [K^{\mp}\pi^{\pm}\pi^0]_D h^{\mp}$, for $h = K$ and π. In both cases the suppressed modes are as yet unobserved, although Belle has reported first evidence for $B^{\mp} \to [\pi^{\mp}K^{\pm}\pi^0]_D K^{\mp}$ and $B^{\mp} \to [\pi^{\mp}K^{\pm}\pi^0]_D \pi^{\mp}$ [20]. As is customary in an ADS analysis, the ratio

$$R_{\mathrm{ADS}(h)}^{K\pi\pi^0}$$
$$\equiv \frac{\Gamma(B^- \to [\pi^-K^+\pi^0]_D h^-) + \Gamma(B^+ \to [\pi^+K^-\pi^0]_D h^+)}{\Gamma(B^- \to [K^-\pi^+\pi^0]_D h^-) + \Gamma(B^+ \to [K^+\pi^-\pi^0]_D h^+)}$$
(1)

is defined to give the relative rates of the suppressed to the favored decays. The asymmetry

$$A_{\mathrm{ADS}(h)}^{K\pi\pi^0}$$
$$\equiv \frac{\Gamma(B^- \to [\pi^-K^+\pi^0]_D h^-) - \Gamma(B^+ \to [\pi^+K^-\pi^0]_D h^+)}{\Gamma(B^- \to [\pi^-K^+\pi^0]_D h^-) + \Gamma(B^+ \to [\pi^+K^-\pi^0]_D h^+)}$$
(2)

quantifies the amount of CP violation in the suppressed modes. An asymmetry is also constructed for the favored channels,

$$A_K^{K\pi\pi^0}$$
$$\equiv \frac{\Gamma(B^- \to [K^-\pi^+\pi^0]_D K^-) - \Gamma(B^+ \to [K^+\pi^-\pi^0]_D K^+)}{\Gamma(B^- \to [K^-\pi^+\pi^0]_D K^-) + \Gamma(B^+ \to [K^+\pi^-\pi^0]_D K^+)}.$$
(3)

The observables $R_{\mathrm{ADS}(K)}^{K\pi\pi^0}$ and $A_{\mathrm{ADS}(K)}^{K\pi\pi^0}$ carry the highest sensitivity to the angle γ; they depend on the underlying physics parameters as

$$R_{\mathrm{ADS}(K)}^{K\pi\pi^0} \approx (r_B)^2 + (r_D^{K\pi\pi^0})^2$$
$$+ 2\kappa_D^{K\pi\pi^0} r_B r_D^{K\pi\pi^0} \cos(\delta_B + \delta_D^{K\pi\pi^0}) \cos\gamma, \quad (4)$$

$$A_{\mathrm{ADS}(K)}^{K\pi\pi^0} \approx [2\kappa_D^{K\pi\pi^0} r_B r_D^{K\pi\pi^0} \sin(\delta_B + \delta_D^{K\pi\pi^0}) \sin\gamma]/R_{\mathrm{ADS}(K)}^{K\pi\pi^0}.$$
(5)

Here $r_D^{K\pi\pi^0} \sim 0.05$ [5] is the ratio of the magnitudes of the doubly Cabibbo-suppressed and Cabibbo-favored D decay amplitudes and $\delta_D^{K\pi\pi^0}$ is the strong-phase difference between the amplitudes, averaged over phase space. The coherence factor $\kappa_D^{K\pi\pi^0}$ accounts for possible dilution effects in the interference arising from the contribution of the intermediate resonances in the D decay [14]. Both $\delta_D^{K\pi\pi^0}$ and $\kappa_D^{K\pi\pi^0}$ have been measured with quantum-correlated $D\bar{D}$ decays collected at the $\psi(3770)$ resonance by the CLEO-c experiment, and have been found to be $(164^{+20}_{-14})^{\circ}$ and 0.82 ± 0.07, respectively [15], where the phase-difference $\delta_D^{K\pi\pi^0}$ is given in the convention where $CP|D^0\rangle = |\bar{D}^0\rangle$. The relatively large value of $\kappa_D^{K\pi\pi^0}$ means that the dilution effects are small and, hence, this decay is a promising mode to exploit for the measurement of γ. Note that for reasons of clarity Eqs. (4) and (5) are restricted to terms of $\mathcal{O}((r_B)^2, (r_D^{K\pi\pi^0})^2, (r_B r_D^{K\pi\pi^0}))$, and the small effects of $D^0\bar{D}^0$ mixing are omitted. Full expressions may be found in Ref. [22].

In the qGLW analysis of the two self-conjugate modes $D \to h'^+h'^-\pi^0$ $(h' = K, \pi)$, observables are defined analogously to those used in the CP-eigenstate case. The first of these is the ratio of partial widths,

$$R_{\mathrm{qGLW}}^{h'h'\pi^0} \equiv \frac{\Gamma(B^- \to D_{F_+^{h'h'\pi^0}} K^-) + \Gamma(B^+ \to D_{F_+^{h'h'\pi^0}} K^+)}{\Gamma(B^- \to D^0 K^-) + \Gamma(B^+ \to \bar{D}^0 K^+)},$$
(6)

where $D_{F_+^{h'h'\pi^0}}$ signifies a D meson with fractional CP-even content $F_+^{h'h'\pi^0}$. Both the numerator and the denominator of Eq. (6) involve B meson partial widths only and have no dependence on the D meson branching fractions. In practice, therefore, $R_{\mathrm{qGLW}}^{h'h'\pi^0}$ is determined by forming the ratio of two more ratios,

$$R_{\mathrm{qGLW}}^{h'h'\pi^0} \approx R_{K/\pi}^{h'h'\pi^0}/R_{K/\pi}^{K\pi\pi^0}, \quad (7)$$

$$R_{K/\pi}^{h'h'\pi^0} \equiv \frac{\Gamma(B^- \to [h'h'\pi^0]_D K^-) + \Gamma(B^+ \to [h'h'\pi^0]_D K^+)}{\Gamma(B^- \to [h'h'\pi^0]_D \pi^-) + \Gamma(B^+ \to [h'h'\pi^0]_D \pi^+)},$$
(8)

$$R_{K/\pi}^{K\pi\pi^0}$$
$$\equiv \frac{\Gamma(B^- \to [K^-\pi^+\pi^0]_D K^-) + \Gamma(B^+ \to [K^+\pi^-\pi^0]_D K^+)}{\Gamma(B^- \to [K^-\pi^+\pi^0]_D \pi^-) + \Gamma(B^+ \to [K^+\pi^-\pi^0]_D \pi^+)},$$
(9)

where the approximate equality in Eq. (7) acknowledges that very small interference effects in the $B^{\mp} \to D\pi^{\mp}$ decays specified in Eqs. (8) and (9) can be neglected. This is a good assumption because the ratio between interfering amplitudes in $B^{\mp} \to D\pi^{\mp}$ decays is known to be very small [4]. Furthermore, the ratio $R_{K/\pi}^{h'h'\pi^0}/R_{K/\pi}^{K\pi\pi^0}$ may be interpreted in terms of the underlying physics parameters, taking these interference effects into account. Asymmetries, $A_{\mathrm{qGLW}(h)}^{h'h'\pi^0}$ $(h = K, \pi)$, are also constructed, where

$$
\begin{aligned}
&A_{\mathrm{qGLW}(h)}^{h'h'\pi^0} \\
&\equiv \frac{\Gamma(B^- \to [h'h'\pi^0]_D h^-) - \Gamma(B^+ \to [h'h'\pi^0]_D h^+)}{\Gamma(B^- \to [h'h'\pi^0]_D h^-) + \Gamma(B^+ \to [h'h'\pi^0]_D h^+)}.
\end{aligned}
\tag{10}
$$

The relations between $R_{\mathrm{qGLW}}^{h'h'\pi^0}$ and $A_{\mathrm{qGLW}(K)}^{h'h'\pi^0}$, the most sensitive to γ of the two asymmetries, and the underlying physics parameters are

$$
R_{\mathrm{qGLW}}^{h'h'\pi^0} = 1 + (r_B)^2 + (2F_+^{h'h'\pi^0} - 1)2r_B \cos \delta_B \cos \gamma, \tag{11}
$$

$$
A_{\mathrm{qGLW}(K)}^{h'h'\pi^0} = (2F_+^{h'h'\pi^0} - 1)2r_B \sin \delta_B \sin \gamma / R_{\mathrm{qGLW}}^{h'h'\pi^0}. \tag{12}
$$

The small effects of $D^0 \bar{D}^0$ mixing are neglected, but can be accommodated if required [18]. A recent analysis using CLEO-c data [18] has used decays of coherently produced $D\bar{D}$ pairs to determine $F_+^{\pi^+\pi^-\pi^0} = 0.968 \pm 0.018$ and $F_+^{K^+K^-\pi^0} = 0.731 \pm 0.062$. The high value of $F_+^{\pi^+\pi^-\pi^0}$ implies that the decay $D^0 \to \pi^+\pi^-\pi^0$ is very close to being a *CP*-even eigenstate and the interference terms in Eqs. (11) and (12) suffer very little dilution, tending towards the equivalent GLW *CP*-even expressions.

When measuring *CP* asymmetries at the LHC, it is necessary to allow for the possibility that the initial state may contain different numbers of B^- and B^+ mesons. Therefore, a production asymmetry,

$$
A_{\mathrm{Prod}} \equiv \frac{\sigma(B^-) - \sigma(B^+)}{\sigma(B^-) + \sigma(B^+)}, \tag{13}
$$

is defined where $\sigma(B^-)$ and $\sigma(B^+)$ are the cross sections for the production of B^- and B^+ mesons, respectively, within the LHCb acceptance.

To summarize, twelve observables are measured in total: the two ADS asymmetries $A_{\mathrm{ADS}(h)}^{K\pi\pi^0}$, two ratios $R_{\mathrm{ADS}(h)}^{K\pi\pi^0}$ and the asymmetry $A_K^{K\pi\pi^0}$; the four qGLW asymmetries $A_{\mathrm{qGLW}(h)}^{h'h'\pi^0}$ and two ratios $R_{\mathrm{qGLW}}^{h'h'\pi^0}$; and the B^+/B^- production asymmetry, A_{Prod}.

III. THE LHCb DETECTOR AND DATA SET

The analysis uses data collected by LHCb in pp collisions at $\sqrt{s} = 7$ TeV in 2011 and 8 TeV in 2012, corresponding to integrated luminosities of 1.0 fb^{-1} and 2.0 fb^{-1}, respectively. The LHCb detector [23,24] is a single-arm forward spectrometer covering the pseudorapidity range $2 < \eta < 5$, designed for the study of particles containing b or c quarks. The detector includes a high-precision tracking system consisting of a silicon-strip vertex detector surrounding the pp interaction region, a large-area silicon-strip detector located upstream of a dipole magnet with a bending power of about 4 Tm, and three stations of silicon-strip detectors and straw drift tubes placed downstream of the magnet. The polarity of the dipole magnet is reversed periodically throughout data-taking in order to combat systematic biases due to possible detector asymmetries. The tracking system provides a measurement of momentum, p, of charged particles with a relative uncertainty that varies from 0.5% at low momentum to 1.0% at 200 GeV/c. The minimum distance of a track to a primary vertex (PV), the impact parameter, is measured with a resolution of $(15 + 29/p_{\mathrm{T}})$ μm, where p_{T} is the component of the momentum transverse to the beam, in GeV/c. Different types of charged hadrons are distinguished using information from two ring-imaging Cherenkov detectors. Photons, electrons and hadrons are identified by a calorimeter system consisting of scintillating-pad and preshower detectors, an electromagnetic calorimeter and a hadronic calorimeter. Muons are identified by a system composed of alternating layers of iron and multiwire proportional chambers. The online event selection is performed by a trigger [25], which consists of a hardware stage, based on information from the calorimeter and muon systems, followed by a software stage, which applies a full event reconstruction. Off-line a loose selection based on a decision tree algorithm [26] is run to reduce the size of the sample prior to final analysis.

Approximately one million simulated events (after geometric detector acceptance) of each class of signal decay are used in the analysis, as well as a large inclusive sample of generic $B_q \to DX$ decays, where $q \in \{u, d, s\}$. In the simulation, pp collisions are generated using PYTHIA [27] with a specific LHCb configuration [28]. Decays of hadronic particles are described by EVTGEN [29], in which final-state radiation is generated using PHOTOS [30]. The interaction of the generated particles with the detector, and its response, are implemented using the GEANT4 toolkit [31] as described in Ref. [32].

IV. CANDIDATE SELECTION

The events used in the analysis must be selected by the hardware trigger, either for the case where the $B^{\mp}$ candidate triggered the event via the hadronic calorimeter (and not the muon system), or where the event was triggered

independently of the $B^{\mp}$ candidate. The study is performed with $B^{\mp} \to Dh^{\mp}$ candidates, where the D meson decays to a three-body final state composed of any combination of two charged kaons and pions and a π^0 candidate. The π^0 is identified by a decay to two photons, as recorded by the electromagnetic calorimeter.

All candidates passing the $B^{\mp} \to Dh^{\mp}$ reconstruction are required to have an invariant mass in the range of $5080-5900$ MeV/c^2. The mass of the reconstructed D candidate is required to be within ± 50 MeV/c^2 of the nominal D^0 mass [5]. In addition, the mass of the π^0 candidate must be within ± 20 MeV/c^2 of the nominal π^0 mass [5]. Both of these mass windows correspond to approximately plus or minus twice the mass resolution of the respective reconstructed particles. The π^0 candidate must also have a momentum of $p_{\mathrm{T}} > 0.5$ GeV/c and $p > 1.0$ GeV/c. The bachelor particle is required to satisfy $0.5 < p_{\mathrm{T}} < 10$ GeV/c and $5 < p < 100$ GeV/c, while the charged D daughters must have $p_{\mathrm{T}} > 0.25$ GeV/c. In order to improve the resolution of the mass of the $B^{\mp}$ candidate, the decay chain is refitted [33] constraining the positions of the $B^{\mp}$ and D vertices, while at the same time constraining the D candidate to its nominal mass.

In addition to these selection criteria, further background suppression is achieved through the use of a boosted decision tree (BDT) discriminator [34] using the *gradient-boost* algorithm [35]. The BDT is trained using a signal sample of $B^{\mp} \to Dh^{\mp}$ events from simulation and a sample of pure combinatorial background from data with $B^{\mp}$ candidates' invariant mass greater than 5900 MeV/c^2, which are not used in the invariant mass fit. The BDT utilizes a variety of properties associated to each signal candidate. These properties include: p and p_{T} of the D meson, the D daughter candidates and the bachelor particle; and the χ^2_{IP} of the D meson, charged D daughter candidates, bachelor particle and the $B^{\mp}$ meson (where χ^2_{IP} is defined as the difference between the χ^2 of the PV reconstructed with and without the particle of interest). Other properties include: the flight distance from the PV for the $B^{\mp}$ and D candidates; vertex quality, χ^2 per degree of freedom, for the $B^{\mp}$ and D candidates; and the angle between the line connecting the PV to the particle's decay vertex and the particle's momentum vector for the $B^{\mp}$ and D candidates. Another characteristic used in the BDT is an isolation variable representative of the p_{T} imbalance surrounding a $B^{\mp}$ candidate. The variable is defined as

$$A_{p_{\mathrm{T}}} = \frac{p_{\mathrm{T}}(B^{\mp}) - \sum_n p_{\mathrm{T}}}{p_{\mathrm{T}}(B^{\mp}) + \sum_n p_{\mathrm{T}}}, \qquad (14)$$

where the sum is performed over the n tracks lying within a cone around the candidate, excluding the tracks related to the signal. The cone is defined by a circle of radius 1.5 units in the plane of pseudorapidity and azimuthal angle (measured in radians). No particle identification (PID)

information is used as an input variable; consequently the BDT has similar performance for both the $B^{\mp} \to DK^{\mp}$ and $B^{\mp} \to D\pi^{\mp}$ decay modes, with some slight variation arising due to differences in kinematics between the two.

The optimal cut value of the BDT is determined by optimizing the metric $s/\sqrt{s+b}$, where s is the expected signal yield in the suppressed $B^{\mp} \to DK^{\mp}$ ADS mode and b is the combinatoric background level as taken from the favored mode, which is expected to have comparable background levels to the suppressed mode. The expected signal yield is calculated as the yield in the favored $B^{\mp} \to D\pi^{\mp}$ ADS mode scaled by the predicted branching fraction of the $B^{\mp} \to DK^{\mp}$ mode and by the expected ratio between the suppressed and favored ADS modes, while taking into account differences in PID efficiency. Assessment of this $s/\sqrt{s+b}$ metric finds a working point where a signal efficiency of 85% is expected while rejecting $>99\%$ of combinatorial background. A similar optimization procedure performed using the $B^{\mp} \to [\pi^+\pi^-\pi^0]_D K^{\mp}$ and $B^{\mp} \to [K^+K^-\pi^0]_D K^{\mp}$ decays returns a comparable working point and, thus, the same requirement is imposed in the selection of the qGLW modes, as well as the ADS modes.

Particle identification, essential for the distinction between $B^{\mp} \to DK^{\mp}$ and $B^{\mp} \to D\pi^{\mp}$ candidates, is quantified by differences between the logarithm of likelihoods, $\ln \mathcal{L}_h$, under five separate mass hypotheses, $h \in \{e, \mu, \pi, K, p\}$ (DLL). For the daughters from the D candidate, the kaon must satisfy $\mathrm{DLL}_{K\pi} \equiv \ln \mathcal{L}_K - \ln \mathcal{L}_\pi > 2$, while the charged pion is required to satisfy $\mathrm{DLL}_{K\pi} < -2$. Candidates with a bachelor having $\mathrm{DLL}_{K\pi} > 4$ are selected into the $B^{\mp} \to DK^{\mp}$ sample (they are said to have *passed* the PID requirement) while those that do not are placed in the $B^{\mp} \to D\pi^{\mp}$ sample (they are said to have *failed* the PID requirement).

Additional restrictions are imposed after the BDT and the PID requirements in order to remove specific sources of background. Contributions from genuine $B^{\mp}$ decays that do not include a D meson are suppressed through a selection requirement on the flight distance significance, FD_D, defined as the distance between the $B^{\mp}$ and D candidate vertices, divided by the uncertainty on this measurement. A requirement of $\mathrm{FD}_D > 2$ is applied. The total branching fractions of $B^{\mp}$ to four-body charmless states with a π^0 are currently unmeasured and their contribution is estimated by studying the contamination of three-body charmless modes to the $B^{\mp} \to [K^{\mp}\pi^{\pm}, \pi^{\mp}K^{\pm}]_D h^{\mp}$ spectra and scaling it according to the known branching fractions. The efficiency of the FD_D requirement is evaluated using simulated b-hadron decays to four-body charmless states with a neutral pion. The requirement is found to be 93% effective in the suppression of this background, a value compatible with that seen in data for the three-body charmless states. From these studies, it is determined that the charmless backgrounds contribute 4 ± 1, 1 ± 1, 4 ± 1 and 3 ± 1 candidates to the

summed-by-charge selections of $B^\mp \to [K^\mp \pi^\pm \pi^0]_D h^\mp$, $B^\mp \to [\pi^\mp K^\pm \pi^0]_D h^\mp$, $B^\mp \to [\pi^+ \pi^- \pi^0]_D h^\mp$ and $B^\mp \to [K^+ K^- \pi^0]_D h^\mp$, respectively.

The suppressed $B^\mp \to [\pi^\mp K^\pm \pi^0]_D h^\mp$ decays are subject to potential contamination from $B^\mp \to [\pi^+ \pi^- \pi^0]_D h^\mp$ and $B^\mp \to [K^+ K^- \pi^0]_D h^\mp$ decays where one of the charged pions or kaons from the D candidate is misidentified as a charged kaon or pion, respectively. Studies performed using simulated events demonstrate that such contamination is minimal, contributing 1 ± 1 candidate to each $B^\mp \to [\pi^\mp K^\pm \pi^0]_D h^\mp$ decay mode. Similarly, there is potential cross feed from favored $B^\mp \to [K^\mp \pi^\pm \pi^0]_D h^\mp$ decays in the suppressed ADS signal samples in which a $K^\pm$ and $\pi^\mp$ are doubly misidentified as a $\pi^\pm$ and a $K^\mp$, respectively. This contamination is reduced by vetoing any suppressed candidate whose reconstructed D mass, under the exchange of mass hypotheses between the daughter kaon and charged pion, lies within ± 30 MeV/c^2 of the nominal D mass. Study of the cross-feed contamination in the mass side-bands of the D candidates allows for an estimate of the residual contamination in the signal region. After all selection requirements, this residual cross feed is estimated to be $(3.1 \pm 0.2) \times 10^{-4}$ of the total favored $B^\mp \to [K^\mp \pi^\pm \pi^0]_D h^\mp$ events.

For each event, only one candidate is selected for analysis. In the 3.8% of cases where more than one candidate is present in an event, a choice is made by selecting the candidate with the $B^\mp$ decay vertex with the smallest χ^2 per degree of freedom.

V. INVARIANT MASS FIT

The observables of interest are determined with a binned maximum-likelihood fit to the invariant mass of the selected $B^\mp$ candidates. A total of sixteen disjoint sub-samples (the favored and suppressed ADS modes and the two qGLW modes, separated according to the charge of the bachelor meson, and by the bachelor PID requirement) are fitted simultaneously. The total probability density function (PDF) used in the fit is built from five main sources, described below, representing different categories of candidates in each subsample.

The $B^\mp \to D\pi^\mp$ signal events are modeled through the use of a modified Gaussian function,

$$f(m) \propto \exp\left(\frac{-(m-\mu)^2}{2\sigma^2 + (m-\mu)^2 \alpha_{L,R}}\right). \qquad (15)$$

This expression describes an asymmetric peak of mean μ and width σ where the values of $\alpha_L (m < \mu)$ and $\alpha_R (m > \mu)$ parametrize the tails of the distribution to the left and to the right of the peak, respectively. These signal events originate from subsamples that fail the bachelor PID requirement for charged kaons. Genuine $B^\mp \to D\pi^\mp$ candidates that pass the PID requirement are

reconstructed as $B^\mp \to DK^\mp$. Since these candidates are reconstructed under an incorrect mass hypothesis, they represent a displaced mass peak with a tail that extends to higher invariant mass. Such misidentified candidates are modeled by the sum of two Gaussian functions, modified to include tail components similar to that of Eq. (15). The two modified Gaussian functions share a mean, but have two separate width parameters that are permitted to float. For the signal peaks, all of the parameters are permitted to vary, with the exception of the lower-mass tail, which is fixed to the value found in simulation, to ensure fit stability, and later considered as a source of systematic uncertainty. The same shape is used for B^- and B^+ decays, although the means are allowed to be different. In addition, while the $B^\mp \to [K^\mp \pi^\pm \pi^0]_D h^\mp$ and $B^\mp \to [\pi^\mp K^\pm \pi^0]_D h^\mp$ signal shapes share the same width, this parameter is permitted to vary for the $B^\mp \to [K^+ K^- \pi^0]_D h^\mp$ and $B^\mp \to [\pi^+ \pi^- \pi^0]_D h^\mp$ modes.

The $B^\mp \to DK^\mp$ signal events, from the subsamples that pass the PID requirement on the bachelor, are modeled using the same modified Gaussian function of Eq. (15). All of the shape parameters are identical to those of the $B^\mp \to D\pi^\mp$ modes, except for the width, which is fixed at $(95 \pm 2)\%$ of that of the $B^\mp \to D\pi^\mp$ modes, based upon studies made using simulated events. Genuine $B^\mp \to DK^\mp$ candidates that fail the PID selection (and thus represent misidentified $B^\mp \to D\pi^\mp$ events) are described using a fixed shape from simulation that is later varied to assign a systematic uncertainty.

Partially reconstructed b-hadron decays are found in the invariant mass region below the $B^\mp$ mass. However, a portion may enter the signal region. Of particular concern are $B^\mp$ ($\overset{(-)}{B}{}^0$) decays involving a neutral (charged) D^* meson, where the D^* decays to a $\overset{(-)}{D}{}^0$ and a neutral (charged) pion with this latter particle missed in reconstruction, leading to the same final state as in the channels of interest. The $\overset{(-)}{D}{}^{*0}$ may also decay via the $\overset{(-)}{D}{}^{*0} \to \overset{(-)}{D}{}^0 \gamma$ channel. When the γ is missed in reconstruction, such decays may also mimic the desired signal candidates. There are also further contributions from $B^\mp$ ($\overset{(-)}{B}{}^0$) decays to $\overset{(-)}{D}{}^0$ and a neutral (charged) ρ or K^*, where the vector meson decays into an $h^\pm \pi^\mp$ ($h^\pm \pi^0$) state from which the $\pi^\mp$ (π^0) is missed in reconstruction. These partially reconstructed decays are described by parabolic functions representative of the decays in question, that have been convolved with a double Gaussian to account for detector resolution. The yields of these background components vary independently in the fit, with no assumption of *CP* symmetry. Additionally, partially reconstructed $\overset{(-)}{B}{}_s{}^0 \to DK^\mp \pi^\pm$ decays and their charge-conjugated

TABLE I.   The final signal yields, split in categories based on the charges of the B hadron (only statistical uncertainties are shown).

B^- decay channel	Yield
$B^- \to [K^-\pi^+\pi^0]_D\pi^-$	18854 ± 176
$B^- \to [K^-\pi^+\pi^0]_DK^-$	1478 ± 39
$B^- \to [\pi^-K^+\pi^0]_D\pi^-$	63 ± 13
$B^- \to [\pi^-K^+\pi^0]_DK^-$	16 ± 9
$B^- \to [\pi^+\pi^-\pi^0]_D\pi^-$	1716 ± 55
$B^- \to [\pi^+\pi^-\pi^0]_DK^-$	139 ± 19
$B^- \to [K^+K^-\pi^0]_D\pi^-$	509 ± 34
$B^- \to [K^+K^-\pi^0]_DK^-$	49 ± 12

B^+ decay channel	Yield
$B^+ \to [K^+\pi^-\pi^0]_D\pi^+$	18882 ± 176
$B^+ \to [K^+\pi^-\pi^0]_DK^+$	1442 ± 39
$B^+ \to [\pi^+K^-\pi^0]_D\pi^+$	25 ± 13
$B^+ \to [\pi^+K^-\pi^0]_DK^+$	24 ± 9
$B^+ \to [\pi^+\pi^-\pi^0]_D\pi^+$	1772 ± 55
$B^+ \to [\pi^+\pi^-\pi^0]_DK^+$	125 ± 19
$B^+ \to [K^+K^-\pi^0]_D\pi^+$	541 ± 34
$B^+ \to [K^+K^-\pi^0]_DK^+$	27 ± 12

modes are considered as background sources to the ADS $B^\mp \to Dh^\mp$ modes. PDFs for this background are determined from simulation and fixed in the invariant mass fit. The $\overset{(-)}{B_s}{}^0$ yields are permitted to float, but CP symmetry is assumed given the limited interference effects due to Cabibbo suppression.

Wrongly reconstructed D meson decays are a source of background under the signal peaks. These are primarily decays where the π^0 candidate is not a daughter of the D meson, but is wrongly assigned as such. In the final fits, these contributions are modeled using a modified Gaussian function with a tail parameter, where this component and the width are permitted to vary, but the mean is fixed based on a study in data. In this study, a binned-maximum likelihood fit is performed to the D mass distribution in a region of $\pm 250 \text{ MeV}/c^2$ about the nominal D mass [5], where the signal and background contributions are modeled separately. The sPlot method [36] is used to assign signal and background weights to the candidates and the $B^\mp$ invariant mass distribution is then plotted using the background weights in order to ascertain how the wrongly reconstructed D background contribution distributes itself in the $B^\mp$ mass spectrum. This study indicates that the background can be described by using the function of Eq. (15) with a single tail parameter. As such, in the final fits, the wrongly reconstructed D meson background is modeled as a fully floating modified Gaussian function, except for the mean that is fixed. The value of the fixed parameter is varied in order to assess a systematic uncertainty.

A linear approximation is adequate to describe the distribution of combinatorial background across the relevant invariant mass spectrum. All $B^\mp \to DK^\mp$ modes and all $B^\mp \to D\pi^\mp$ modes share the same respective shapes, though yields vary independently. This allows for greater fit stability as the low statistics modes share fit information from the higher statistics modes.
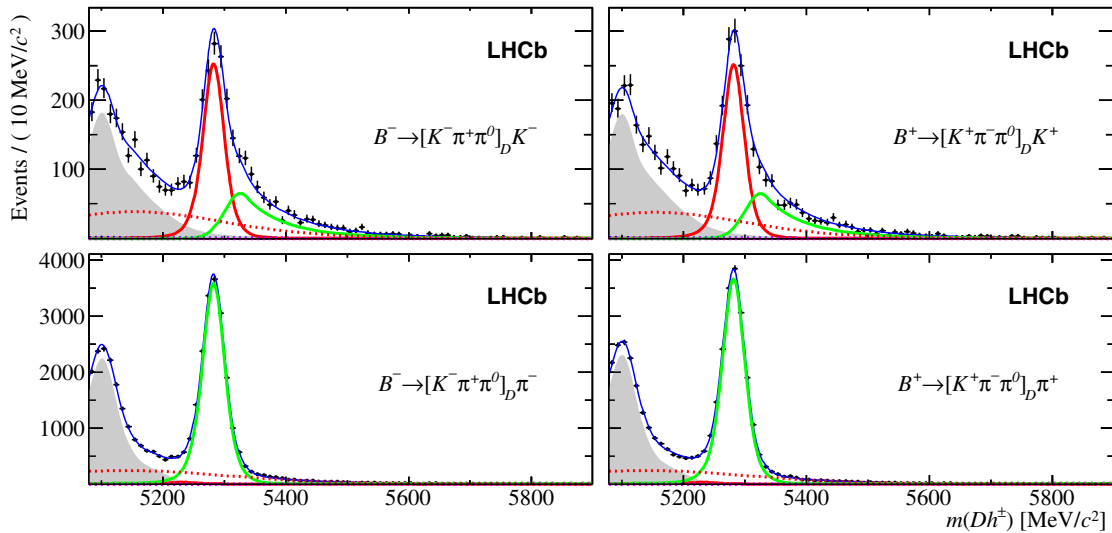

FIG. 1 (color online).   Invariant mass distributions of selected $B^\mp \to [K^\mp\pi^\pm\pi^0]_Dh^\mp$ candidates, separated by B hadron charge. $B^\mp \to DK^\mp$ signal events are in the upper plots and $B^\mp \to D\pi^\mp$ events are in the lower plots. The solid dark (red) curve represents $B^\mp \to DK^\mp$ events and the solid light (green) curve represents $B^\mp \to D\pi^\mp$ events. The solid (grey) shape indicates partially reconstructed $B^\mp$ decays and the heavy dotted (red) curve indicates wrongly reconstructed D decays. The solid (blue) line represents the total PDF and includes the combinatorial component.
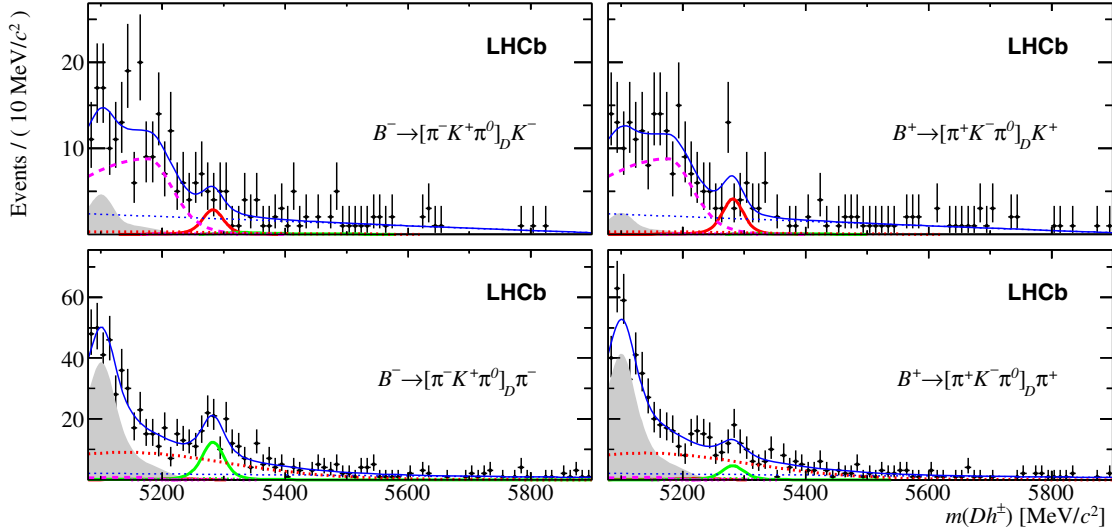
FIG. 2 (color online).   Invariant mass distributions of selected $B^{\mp} \to [\pi^{\mp}K^{\pm}\pi^0]_D h^{\mp}$ candidates. See the caption of Fig. 1 for a full description. The lightly dotted (blue) line represents the combinatorial component and the long-dashed (magenta) line indicates contributions from partially reconstructed $B_s^0 \to DK^{\mp}\pi^{\pm}$ decays where the pion is not reconstructed.

The measured signal yields allow the fit to determine the observables of interest. For example, the relationship between $n_{\pi K \pi^0}^{DK+}$, the yield of the decay $B^+ \to [\pi^+K^-\pi^0]_D K^+$, and the physics observables is given by

$$n_{\pi K \pi^0}^{DK+} = \frac{n_{K\pi\pi^0}^{D\pi} \cdot R_{K/\pi}^{K\pi\pi^0} \cdot R_{\mathrm{ADS}(K)}^{K\pi\pi^0} \cdot \epsilon_{\mathrm{exp}}}{1 + \left[\frac{1 + A_{\mathrm{ADS}(K)}^{K\pi\pi^0}}{1 - A_{\mathrm{ADS}(K)}^{K\pi\pi^0}} \cdot \frac{1 + A_{\mathrm{Prod}}}{1 - A_{\mathrm{Prod}}} \cdot \frac{1 + A_{\mathrm{det}}}{1 - A_{\mathrm{det}}}\right]}, \qquad (16)$$

where ϵ_{exp} represents experimental selection efficiency effects and A_{det} are detector-related asymmetries (both of these are further discussed in Sec. VI) and $n_{K\pi\pi^0}^{D\pi}$ is the total yield of $B^{\mp} \to [K^{\mp}\pi^{\pm}\pi^0]_D \pi^{\mp}$ decays. In the fit, an analogous expression to Eq. (16) is used for the corresponding B^- decay as well as comparable equations for the other decay modes and their associated *CP* observables.

The fit is performed such that all of the observables defined by Eqs. (1), (2), (3), (8), (10) and (13) are free parameters. The signal yields for the decay modes of interest are presented in Table I. The uncertainties are statistical only; the systematic uncertainties are discussed in Sec. VI. The corresponding invariant mass spectra, separated by the charge of the $B^{\mp}$ candidate, are presented in Figs. 1, 2, 3 and 4.
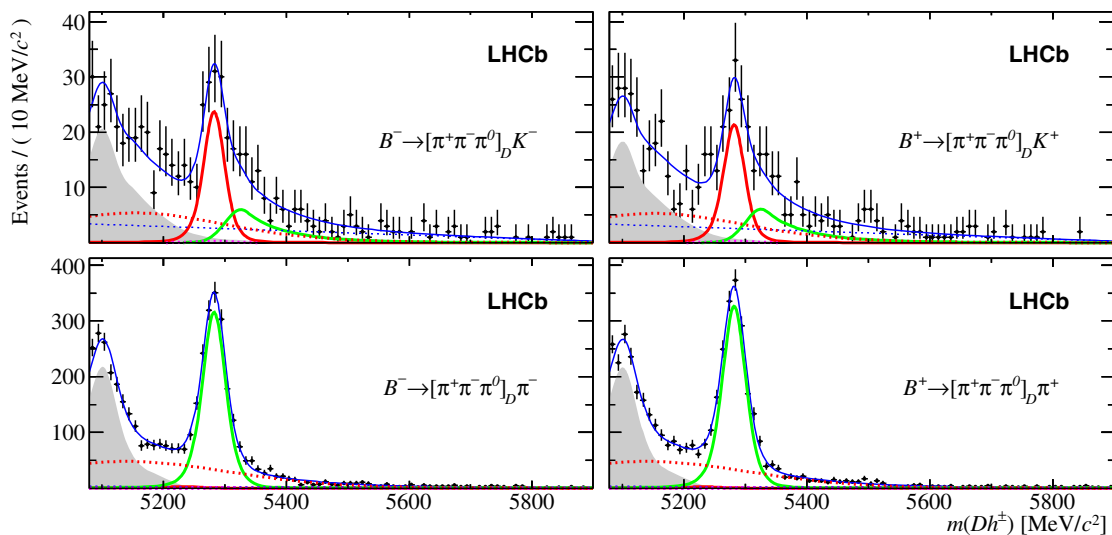

FIG. 3 (color online).   Invariant mass distributions of selected $B^{\mp} \to [\pi^+\pi^-\pi^0]_D h^{\mp}$ candidates. See the caption of Fig. 1 for a full description. The lightly dotted (blue) line represents the combinatorial component.
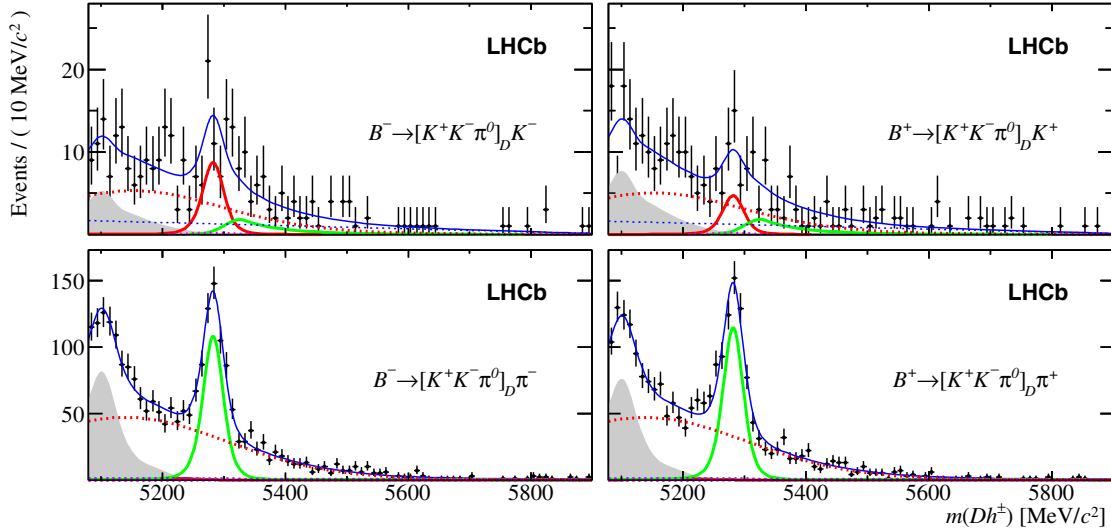
FIG. 4 (color online). Invariant mass distributions of selected $B^{\mp} \rightarrow [K^+K^-\pi^0]_D h^{\mp}$ candidates. See the caption of Fig. 1 for a full description. The lightly dotted (blue) line represents the combinatorial component.

VI. SYSTEMATIC UNCERTAINTIES AND RESULTS

In addition to the sources of systematic uncertainties originating from fixed PDF parameters in the fit, there are several other sources that are considered. In the favored and suppressed ADS modes, the ratio $R_{K/\pi}^{K\pi\pi^0}$ is fixed at 7.74% based on the measurement performed in Ref. [8] and is assigned a systematic uncertainty of 0.22%, as per the uncertainties of that analysis. The $B^{\mp} \rightarrow DK^{\mp}$ versus $B^{\mp} \rightarrow D\pi^{\mp}$ ratio, however, is permitted to vary in the $B^{\mp} \rightarrow [\pi^+\pi^-\pi^0]_D h^{\mp}$ and $B^{\mp} \rightarrow [K^+K^-\pi^0]_D h^{\mp}$ analyses as it must be measured for each mode in order to determine the $R_{\text{qGLW}}^{h'h'\pi^0}$ observables.

The proportion of $B^{\mp} \rightarrow Dh^{\mp}$ samples passing or failing the PID requirements is determined from a sample of more than 100 million $D^{*\pm}$ decays reconstructed as $D^{*\pm} \rightarrow D\pi^{\pm}$, $D \rightarrow K^{\mp}\pi^{\pm}$. This reconstruction is performed entirely using kinematic variables and provides a high-purity calibration sample of $K^{\pm}$ and $\pi^{\pm}$ tracks. The PID efficiency varies as a function of track momentum, pseudorapidity and detector occupancy [37]. The average PID efficiency of the signal is determined by reweighting the calibration spectra in these variables to those of the candidates in the favored ADS sample. This average PID efficiency is evaluated to be 84.5% and 96.3% for kaons and pions, respectively. Systematic uncertainties of 0.5% and 0.8% for bachelor pions and bachelor kaons, respectively, are assigned to the efficiencies, which arise from the reweighting procedure.

Due to differences in interactions with the detector material, a small negative asymmetry is expected in the detection of K^- and K^+ mesons. An asymmetry for pions may also be present and is assigned a value of $(0.0 \pm 0.3)\%$ [38]. The difference between the kaon and pion detection asymmetries is taken to be $-(1.1 \pm 0.4)\%$ from studies performed in Ref. [39]. These asymmetry values also account for the physical asymmetry of the left and right sides of the detector, after summing the data sets from both magnet polarities. There is no systematic uncertainty associated with the possible difference in number of B^- and B^+ mesons, since the production asymmetry A_{Prod} is a variable parameter in the fit.

The measured observables in the analysis are related to the ratio of relative efficiencies between the $B^{\mp} \rightarrow DK^{\mp}$ and $B^{\mp} \rightarrow D\pi^{\mp}$ modes, $\epsilon_{B\rightarrow DK}/\epsilon_{B\rightarrow D\pi}$, independent of PID effects. These ratios relate the efficiency differences due to trigger, reconstruction and selection effects. They are measured in simulation to be $(97.5 \pm 3.4)\%$ for the $B^{\mp} \rightarrow [K^{\mp}\pi^{\pm}\pi^0]_D h^{\mp}$ and $B^{\mp} \rightarrow [\pi^{\mp}K^{\pm}\pi^0]_D h^{\mp}$ modes, $(95.7 \pm 2.8)\%$ for the $B^{\mp} \rightarrow [\pi^+\pi^-\pi^0]_D h^{\mp}$ modes and $(98.9 \pm 2.8)\%$ for the $B^{\mp} \rightarrow [K^+K^-\pi^0]_D h^{\mp}$ modes. The uncertainties listed are based on the finite size of the simulated samples and account for the imperfect modeling of pion and kaon absorption rates in the detector material.

In order to estimate the systematic uncertainties from the sources described in this section and in Sec. V, the fit is performed many times, varying each source by its assigned uncertainty, under the assumption that the uncertainty is Gaussian distributed. The spread (RMS) in the distribution of the fitted value of the observables is taken as the systematic uncertainty. These uncertainties are summarized in Table II.

The values for the coherence factor, average strong-phase differences and CP-even fraction reported in Refs. [15] and [18] assume a uniform acceptance across the three-body phase space of the D decay, which is not the case in this analysis. Studies are performed with amplitude models for the decays of interest and a modeling of the

TABLE II. Systematic uncertainties on the observables, multiplied by a factor of 10^3. "PID" refers to the fixed PID efficiency attributed to the bachelor tracks. "PDFs" refers to the uncertainties based on fixed parameters in the PDF shapes that are used in the invariant mass fit. "Sim" refers to the use of simulation to calculate relative efficiencies between the $B^{\mp} \to DK^{\mp}$ and $B^{\mp} \to D\pi^{\mp}$ modes, in addition to the estimated charmless background contributions and the fixed DK to $D\pi$ ratio on the ADS modes. "A_{instr}" refers to the interaction and detection asymmetries. The "Total" column represents the sum in quadrature of all of the categories of systematic uncertainties.

	PID	PDFs	Sim	A_{instr}	Total
$A_{\text{ADS}(K)}^{K\pi\pi^0}$	3.4	39.6	8.7	5.7	41.1
$A_{\text{ADS}(\pi)}^{K\pi\pi^0}$	1.6	7.5	4.5	6.9	11.3
$A_{\text{qGLW}(K)}^{KK\pi^0}$	5.1	10.2	18.8	2.1	22.1
$A_{\text{qGLW}(K)}^{\pi\pi\pi^0}$	0.9	7.9	7.3	0.9	10.8
$A_{\text{qGLW}(\pi)}^{KK\pi^0}$	0.8	2.2	1.2	4.4	5.1
$A_{\text{qGLW}(\pi)}^{\pi\pi\pi^0}$	0.3	0.9	0.7	4.2	4.4
$A_K^{K\pi\pi^0}$	0.4	0.9	1.4	4.2	4.6
$R_{\text{ADS}(K)}^{K\pi\pi^0}$	0.3	2.0	0.6	0.1	2.1
$R_{\text{ADS}(\pi)}^{K\pi\pi^0}$	0.02	0.05	0.02	0.01	0.06
$R_{\text{qGLW}}^{KK\pi^0}$	23.8	24.9	36.5	7.7	50.8
$R_{\text{qGLW}}^{\pi\pi\pi^0}$	8.1	20.7	42.5	5.3	48.3
A_{Prod}	0.3	0.3	0.5	5.0	5.0

acceptance function derived from simulation to assess the impact upon these parameters arising from this source. It is found that in all cases the biases are negligible compared to the assigned uncertainties.

The results for the observables, as determined by the fit, are

$$A_{\text{ADS}(K)}^{K\pi\pi^0} = -0.20 \pm 0.27 \pm 0.04$$

$$A_{\text{ADS}(\pi)}^{K\pi\pi^0} = 0.438 \pm 0.190 \pm 0.011$$

$$A_{\text{qGLW}(K)}^{KK\pi^0} = 0.30 \pm 0.20 \pm 0.02$$

$$A_{\text{qGLW}(K)}^{\pi\pi\pi^0} = 0.054 \pm 0.091 \pm 0.011$$

$$A_{\text{qGLW}(\pi)}^{KK\pi^0} = -0.030 \pm 0.040 \pm 0.005$$

$$A_{\text{qGLW}(\pi)}^{\pi\pi\pi^0} = -0.016 \pm 0.020 \pm 0.004$$

$$A_K^{K\pi\pi^0} = 0.010 \pm 0.026 \pm 0.005$$

$$R_{\text{ADS}(K)}^{K\pi\pi^0} = 0.0140 \pm 0.0047 \pm 0.0021$$

$$R_{\text{ADS}(\pi)}^{K\pi\pi^0} = 0.00235 \pm 0.00049 \pm 0.00006$$

$$R_{\text{qGLW}}^{KK\pi^0} = 0.95 \pm 0.22 \pm 0.05$$

$$R_{\text{qGLW}}^{\pi\pi\pi^0} = 0.98 \pm 0.11 \pm 0.05$$

$$A_{\text{Prod}} = -0.0008 \pm 0.0055 \pm 0.0050,$$

where the first uncertainties are statistical and the second are systematic.

None of the asymmetry observables exhibit any significant *CP* violation. The results for the ADS observables are more precise than those obtained by previous experiments [19,20] and are compatible with them. Furthermore, apart from $A_{\text{qGLW}(K)}^{\pi\pi\pi^0}$, this is the first time that the qGLW observables have been measured.

A likelihood-ratio test is used to assess the significance of the suppressed ADS signal yields, as well as those of the $B^{\mp} \to [K^+K^-\pi^0]_D h^{\mp}$ decays. This is performed by calculating the quantity $\sqrt{-2\ln(\mathcal{L}_b/\mathcal{L}_{s+b})}$ where $\mathcal{L}_b$ and $\mathcal{L}_{s+b}$ are the maximum likelihood values of the background-only and signal-plus-background hypotheses, respectively. Including systematic uncertainties, significances of 5.3σ and 2.8σ are found for the $B^{\mp} \to [\pi^{\mp}K^{\pm}\pi^0]_D\pi^{\mp}$ and $B^{\mp} \to [\pi^{\mp}K^{\pm}\pi^0]_D K^{\mp}$ decays, respectively. For the $B^{\mp} \to [K^+K^-\pi^0]_D h^{\mp}$ selections, the $B^{\mp} \to D\pi^{\mp}$ mode is found to have a significance greater than 10σ, while a significance of 4.5σ is measured for the $B^{\mp} \to DK^{\mp}$ decay.

VII. INTERPRETATION AND CONCLUSIONS

The measured observables from the $B^{\mp} \to DK^{\mp}$ decay channels are used to obtain constraints on the underlying physics parameters r_B, δ_B and γ. For this purpose, the small effects of $D^0\bar{D}^0$ mixing and interference in $B^{\mp} \to D\pi^{\mp}$ decays are neglected. Using the measurements and associated fit covariance matrix and systematic uncertainty
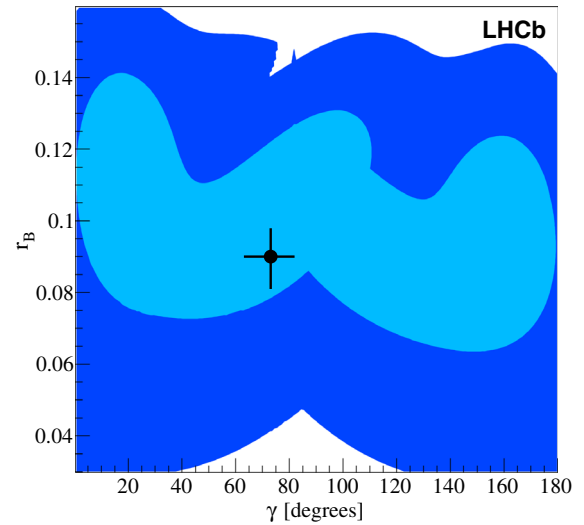

FIG. 5 (color online). Scan of the χ^2 probabilities over the $\gamma - r_B$ parameter space. Shown are the $n\sigma$ profile likelihood contours, where $\Delta\chi^2 = n^2$, with $n = 1$ being the light (blue) shaded region, $n = 2$ the dark (blue) shaded region and $n = 3$ corresponding to the white area. The result is seen to be compatible with the current LHCb measurement of γ and r_B, indicated by the point with error bars.
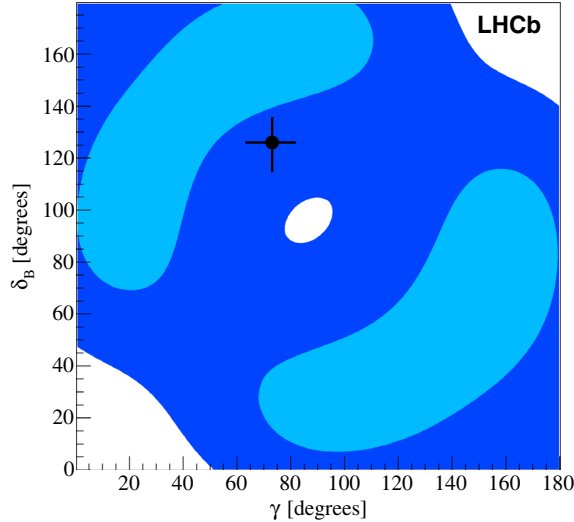
FIG. 6 (color online). Scan of the χ^2 probabilities over the $\gamma - \delta_B$ parameter space. Shown are the $n\sigma$ profile likelihood contours, where $\Delta\chi^2 = n^2$, with $n = 1$ being the light (blue) shaded region, $n = 2$ the dark (blue) shaded region and $n = 3$ corresponding to the white area. The result is compatible with the current LHCb measurement of γ and δ_B, indicated by the point with error bars.

correlations, and taking external measurements of $\kappa_D^{K\pi\pi^0}$, $F_+^{\pi^+\pi^-\pi^0}$ and $F_+^{K^+K^-\pi^0}$ [15,18] and the branching ratios of the D decay channels [5] as additional inputs with their associated uncertainties, a global χ^2 minimization is performed. A scan of the physics parameters is executed for a range of values and the difference in goodness of fit, $\Delta\chi^2$, between the parameter scan values and the global minimum, is evaluated. Assuming that this χ^2 minimization function is distributed in a Gaussian manner enables a probability to be assigned for each set of values of the physics parameters.

Two-dimensional scans are performed for γ vs r_B and γ vs δ_B in the ranges $0.03 < r_B < 0.16$, $0° < \delta_B < 180°$ and $0° < \gamma < 180°$. Figs. 5 and 6 shows the 1σ, 2σ and 3σ contours determined from these scans. It can be seen that the results are compatible with the values obtained from a global analysis of other LHCb measurements sensitive to γ at tree level [4], which are also shown. The scans return a best-fit value for the parameter r_B of 0.11 ± 0.03. No useful constraints are obtained for either γ or δ_B. However, the measurements of the observables are expected to provide improved precision on these parameters when included in a global analysis of all LHCb $B^{\mp} \rightarrow DK^{\mp}$ results.

In summary, measurements of CP asymmetries and related observables have been performed using $B^{\mp} \rightarrow DK^{\mp}$ and $B^{\mp} \rightarrow D\pi^{\mp}$ decays with an inclusive analysis of the ADS modes $D \rightarrow K^{\mp}\pi^{\pm}\pi^0$ and, for the first time, the qGLW modes $D \rightarrow \pi^+\pi^-\pi^0$ and $D \rightarrow K^+K^-\pi^0$. The results for the ADS observables are the most precise measurements of these quantities. No evidence of CP violation is obtained with the current experimental precision. First observations have been made of the decays $B^{\mp} \rightarrow [\pi^{\mp}K^{\pm}\pi^0]_D\pi^{\mp}$ and $B^{\mp} \rightarrow [K^+K^-\pi^0]_D\pi^{\mp}$, and first evidence is obtained for the mode $B^{\mp} \rightarrow [K^+K^-\pi^0]_DK^{\mp}$. When analysed in the context of the underlying physics parameters, the results exhibit good consistency with other LHCb measurements. The measurements will be valuable in improving knowledge of the unitarity triangle angle γ when combined with LHCb results from $B^{\mp} \rightarrow DK^{\mp}$ measurements exploiting other D decay channels.

ACKNOWLEDGMENTS

[1] N. Cabibbo, Unitary Symmetry and Leptonic Decays, Phys. Rev. Lett. **10**, 531 (1963); M. Kobayashi and T. Maskawa, *CP* violation in the renormalizable theory of weak interaction, Prog. Theor. Phys. **49**, 652 (1973).

[2] J. P. Lees *et al.* (BABAR Collaboration), Observation of direct *CP* violation in the measurement of the Cabibbo-Kobayashi-Maskawa angle γ with $B^{\pm} \to D^{(*)} K^{(*)\pm}$ decays, Phys. Rev. D **87**, 052015 (2013).

[3] K. Trabelsi, Study of direct *CP* in charmed B decays and measurement of the CKM angle γ at Belle, arXiv:1301.2033.

[4] R. Aaij *et al.* (LHCb Collaboration), A measurement of the CKM angle γ from a combination of $B^{\pm} \to Dh^{\pm}$ analyses, Phys. Lett. B **726**, 151 (2013); LHCb Collaboration Report No. LHCb-CONF-2014-004.

[5] K. A. Olive *et al.* (Particle Data Group), Review of particle physics, Chin. Phys. C **38**, 090001 (2014).

[6] D. Atwood, I. Dunietz, and A. Soni, Enhanced *CP* Violation with $B \to KD^0(\bar{D}^0)$ Modes and Extraction of the CKM Angle γ, Phys. Rev. Lett. **78**, 3257 (1997); Improved Methods for Observing *CP* Violation in $B^{\pm} \to KD$ and Measuring the CKM Phase γ, Phys. Rev. D **63**, 036005 (2001).

[7] M. Gronau and D. London, How to determine all the angles of the unitarity triangle from $B_d^0 \to DK_S^0$ and $B_s^0 \to D\phi$, Phys. Lett. B **253**, 483 (1991); M. Gronau and D. Wyler, On determining a weak phase from *CP* asymmetries in charged B decays, Phys. Lett. B **265**, 172 (1991).

[8] R. Aaij *et al.* (LHCb Collaboration), Observation of *CP* violation in $B^{\pm} \to DK^{\pm}$ decays, Phys. Lett. B **712**, 203 (2012); **713**, 351(E) (2012).

[9] R. Aaij *et al.* (LHCb Collaboration), Observation of the suppressed ADS modes $B^{\pm} \to [\pi^{\pm} K^{\mp} \pi^+ \pi^-]_D K^{\pm}$ and $B^{\pm} \to [\pi^{\pm} K^{\mp} \pi^+ \pi^-]_D \pi^{\pm}$, Phys. Lett. B **723**, 44 (2013).

[10] R. Aaij *et al.* (LHCb Collaboration), A study of *CP* violation in $B^{\pm} \to DK^{\pm}$ and $B^{\pm} \to D\pi^{\pm}$ decays with $D \to K_S^0 K^{\pm} \pi^{\mp}$ final states, Phys. Lett. B **733**, 36 (2014).

[11] R. Aaij *et al.* (LHCb Collaboration), Measurement of *CP* violation parameters in $B^0 \to DK^{*0}$ decays, Phys. Rev. D **90**, 112002 (2014).

[12] R. Aaij *et al.* (LHCb Collaboration), Measurement of the CKM angle γ using $B^{\pm} \to DK^{\pm}$ with $D \to K_S^0 \pi^+ \pi^-$, $K_S^0 K^+ K^-$ decays, J. High Energy Phys. 10 (2014) 097.

[13] R. Aaij *et al.* (LHCb Collaboration), Measurement of *CP* violation and constraints on the CKM angle γ in $B^{\pm} \to DK^{\pm}$ with $D \to K_S^0 \pi^+ \pi^-$ decays, Nucl. Phys. **B888**, 169 (2014).

[14] D. Atwood and A. Soni, Role of charm factory in extracting CKM phase information via $B \to DK$, Phys. Rev. D **68**, 033003 (2003).

[15] J. Libby *et al.*, New determination of the $D^0 \to K^- \pi^+ \pi^0$ and $D^0 \to K^- \pi^+ \pi^+ \pi^-$ coherence factors and average strong-phase differences, Phys. Lett. B **731**, 197 (2014).

[16] N. Lowrey *et al.* (CLEO Collaboration), Determination of the $D^0 \to K^- \pi^+ \pi^0$ and $D^0 \to K^- \pi^+ \pi^+ \pi^-$ coherence factors and average strong-phase differences using quantum-correlated measurements, Phys. Rev. D **80**, 031105 (2009).

[17] J. Insler *et al.* (CLEO Collaboration), Studies of the decays $D^0 \to K_S^0 K^- \pi^+$ and $D^0 \to K_S^0 K^+ \pi^-$, Phys. Rev. D **85**, 092016 (2012).

[18] M. Nayak, J. Libby, S. Malde, C. Thomas, G. Wilkinson, R. A. Briere, P. Naik, T. Gershon, and G. Bonvicini, First determination of the *CP* content of $D \to \pi^+ \pi^- \pi^0$ and $D \to K^+ K^- \pi^0$, Phys. Lett. B **740**, 1 (2015).

[19] J. P. Lees *et al.* (BABAR Collaboration), Search for $b \to u$ transitions in $B^{\pm} \to [K^{\mp} \pi^{\pm} \pi^0]_D K^{\pm}$ decays, Phys. Rev. D **84**, 012002 (2011).

[20] M. Nayak *et al.* (Belle Collaboration), Evidence for the suppressed decay $B^- \to DK^-$, $D \to K^+ \pi^- \pi^0$, Phys. Rev. D **88**, 091104 (2013).

[21] B. Aubert *et al.* (BABAR Collaboration), Measurement of *CP* Violation Parameters with a Dalitz Plot Analysis of $B^{\pm} \to D(\pi^+ \pi^- \pi^0) K^{\pm}$, Phys. Rev. Lett. **99**, 251801 (2007).

[22] M. Rama, Effect of $D - \bar{D}$ mixing in the extraction of γ with $B \to D^0 K^-$ and $B^- \to D^0 \pi^-$ decays, Phys. Rev. D **89**, 014021 (2014).

[23] A. A. Alves Jr. *et al.* (LHCb Collaboration), The LHCb detector at the LHC, JINST **3**, S08005 (2008).

[24] R. Aaij *et al.* (LHCb Collaboration), LHCb detector performance, Int. J. Mod. Phys. A **30**, 1530022 (2015).

[25] R. Aaij *et al.*, The LHCb trigger and its performance in 2011, JINST **8**, P04022 (2013).

[26] V. V. Gligorov and M. Williams, Efficient, reliable and fast high-level triggering using a bonsai boosted decision tree, JINST **8**, P02013 (2013).

[27] T. Sjöstrand, S. Mrenna, and P. Skands, PYTHIA 6.4 physics and manual, J. High Energy Phys. 05 (2006) 026; A brief introduction to PYTHIA 8.1, Comput. Phys. Commun. **178**, 852 (2008).

[28] I. Belyaev *et al.*, Handling of the generation of primary events in Gauss, the LHCb simulation framework, J. Phys. Conf. Ser. **331**, 032047 (2011).

[29] D. J. Lange, The EvtGen particle decay simulation package, Nucl. Instrum. Methods Phys. Res., Sect A **462**, 152 (2001).

[30] P. Golonka and Z. Was, PHOTOS Monte Carlo: A precision tool for QED corrections in Z and W decays, Eur. Phys. J. C **45**, 97 (2006).

[31] J. Allison *et al.* (Geant4 Collaboration), Geant4 developments and applications, IEEE Trans. Nucl. Sci. **53**, 270 (2006); S. Agostinelli *et al.* (Geant4 Collaboration), Geant4: A simulation toolkit, Nucl. Instrum. Methods Phys. Res., Sect. A **506**, 250 (2003).

[32] M. Clemencic, G. Corti, S. Easo, C. R Jones, S. Miglioranzi, M. Pappagallo, and P. Robbe, The LHCb simulation application, Gauss: Design, evolution and experience, J. Phys. Conf. Ser. **331**, 032023 (2011).

[33] W. D. Hulsbergen, Decay chain fitting with a Kalman filter, Nucl. Instrum. Methods Phys. Res., Sect. A **552**, 566 (2005).

[34] L. Breiman, J. H. Friedman, R. A. Olshen, and C. J. Stone, *Classification and Regression Trees* (Wadsworth International Group, Belmont, CA, 1984).

[35] J. H. Friedman, Stochastic gradient boosting, Computational Statistics and Data Analysis **38**, 367 (2002).

[36] M. Pivk and F. R. Le Diberder, sPlot: A statistical tool to unfold data distributions, Nucl. Instrum. Methods Phys. Res., Sect. A **555**, 356 (2005).

[37] M. Adinolfi *et al.*, Performance of the LHCb RICH detector at the LHC, Eur. Phys. J. C **73**, 2431 (2013).

[38] R. Aaij *et al.* (LHCb Collaboration), Search for *CP* violation in $D^+ \to \phi\pi^+$ and $D_s^+ \to K_S^0\pi^+$ decays, J. High Energy Phys. 06 (2013) 112.

[39] R. Aaij *et al.* (LHCb Collaboration), Measurement of *CP* asymmetry in $D^0 \to K^-K^+$ and $D^0 \to \pi^-\pi^+$ decays, J. High Energy Phys. 07 (2014) 041.

R. Aaij,[38] B. Adeva,[37] M. Adinolfi,[46] A. Affolder,[52] Z. Ajaltouni,[5] S. Akar,[6] J. Albrecht,[9] F. Alessio,[38] M. Alexander,[51] S. Ali,[41] G. Alkhazov,[30] P. Alvarez Cartelle,[53] A. A. Alves Jr,[57] S. Amato,[2] S. Amerio,[22] Y. Amhis,[7] L. An,[3] L. Anderlini,[17,a] J. Anderson,[40] M. Andreotti,[16,b] J. E. Andrews,[58] R. B. Appleby,[54] O. Aquines Gutierrez,[10] F. Archilli,[38] P. d'Argent,[11] A. Artamonov,[35] M. Artuso,[59] E. Aslanides,[6] G. Auriemma,[25,c] M. Baalouch,[5] S. Bachmann,[11] J. J. Back,[48] A. Badalov,[36] C. Baesso,[60] W. Baldini,[16,38] R. J. Barlow,[54] C. Barschel,[38] S. Barsuk,[7] W. Barter,[38] V. Batozskaya,[28] V. Battista,[39] A. Bay,[39] L. Beaucourt,[4] J. Beddow,[51] F. Bedeschi,[23] I. Bediaga,[1] L. J. Bel,[41] I. Belyaev,[31] E. Ben-Haim,[8] G. Bencivenni,[18] S. Benson,[38] J. Benton,[46] A. Berezhnoy,[32] R. Bernet,[40] A. Bertolin,[22] M.-O. Bettler,[38] M. van Beuzekom,[41] A. Bien,[11] S. Bifani,[45] T. Bird,[54] A. Birnkraut,[9] A. Bizzeti,[17,d] T. Blake,[48] F. Blanc,[39] J. Blouw,[10] S. Blusk,[59] V. Bocci,[25] A. Bondar,[34] N. Bondar,[30,38] W. Bonivento,[15] S. Borghi,[54] M. Borsato,[7] T. J. V. Bowcock,[52] E. Bowen,[40] C. Bozzi,[16] S. Braun,[11] D. Brett,[54] M. Britsch,[10] T. Britton,[59] J. Brodzicka,[54] N. H. Brook,[46] A. Bursche,[40] J. Buytaert,[38] S. Cadeddu,[15] R. Calabrese,[16,b] M. Calvi,[20,e] M. Calvo Gomez,[36,f] P. Campana,[18] D. Campora Perez,[38] L. Capriotti,[54] A. Carbone,[14,g] G. Carboni,[24,h] R. Cardinale,[19,i] A. Cardini,[15] P. Carniti,[20] L. Carson,[50] K. Carvalho Akiba,[2,38] R. Casanova Mohr,[36] G. Casse,[52] L. Cassina,[20,e] L. Castillo Garcia,[38] M. Cattaneo,[38] Ch. Cauet,[9] G. Cavallero,[19] R. Cenci,[23,j] M. Charles,[8] Ph. Charpentier,[38] M. Chefdeville,[4] S. Chen,[54] S.-F. Cheung,[55] N. Chiapolini,[40] M. Chrzaszcz,[40,26] X. Cid Vidal,[38] G. Ciezarek,[41] P. E. L. Clarke,[50] M. Clemencic,[38] H. V. Cliff,[47] J. Closier,[38] V. Coco,[38] J. Cogan,[6] E. Cogneras,[5] V. Cogoni,[15,k] L. Cojocariu,[29] G. Collazuol,[22] P. Collins,[38] A. Comerma-Montells,[11] A. Contu,[15,38] A. Cook,[46] M. Coombes,[46] S. Coquereau,[8] G. Corti,[38] M. Corvo,[16,b] B. Couturier,[38] G. A. Cowan,[50] D. C. Craik,[48] A. Crocombe,[48] M. Cruz Torres,[60] S. Cunliffe,[53] R. Currie,[53] C. D'Ambrosio,[38] J. Dalseno,[46] P. N. Y. David,[41] A. Davis,[57] K. De Bruyn,[41] S. De Capua,[54] M. De Cian,[11] J. M. De Miranda,[1] L. De Paula,[2] W. De Silva,[57] P. De Simone,[18] C.-T. Dean,[51] D. Decamp,[4] M. Deckenhoff,[9] L. Del Buono,[8] N. Déléage,[4] D. Derkach,[55] O. Deschamps,[5] F. Dettori,[38] B. Dey,[40] A. Di Canto,[38] F. Di Ruscio,[24] H. Dijkstra,[38] S. Donleavy,[52] F. Dordei,[11] M. Dorigo,[39] A. Dosil Suárez,[37] D. Dossett,[48] A. Dovbnya,[43] K. Dreimanis,[52] L. Dufour,[41] G. Dujany,[54] F. Dupertuis,[39] P. Durante,[38] R. Dzhelyadin,[35] A. Dziurda,[26] A. Dzyuba,[30] S. Easo,[49,38] U. Egede,[53] V. Egorychev,[31] S. Eidelman,[34] S. Eisenhardt,[50] U. Eitschberger,[9] R. Ekelhof,[9] L. Eklund,[51] I. El Rifai,[5] Ch. Elsasser,[40] S. Ely,[59] S. Esen,[11] H. M. Evans,[47] T. Evans,[55] A. Falabella,[14] C. Färber,[11] C. Farinelli,[41] N. Farley,[45] S. Farry,[52] R. Fay,[52] D. Ferguson,[50] V. Fernandez Albor,[37] F. Ferrari,[14] F. Ferreira Rodrigues,[1] M. Ferro-Luzzi,[38] S. Filippov,[33] M. Fiore,[16,38,b] M. Fiorini,[16,b] M. Firlej,[27] C. Fitzpatrick,[39] T. Fiutowski,[27] P. Fol,[53] M. Fontana,[10] F. Fontanelli,[19,i] R. Forty,[38] O. Francisco,[2] M. Frank,[38] C. Frei,[38] M. Frosini,[17] J. Fu,[21] E. Furfaro,[24,h] A. Gallas Torreira,[37] D. Galli,[14,g] S. Gallorini,[22,38] S. Gambetta,[19,i] M. Gandelman,[2] P. Gandini,[55] Y. Gao,[3] J. García Pardiñas,[37] J. Garofoli,[59] J. Garra Tico,[47] L. Garrido,[36] D. Gascon,[36] C. Gaspar,[38] U. Gastaldi,[16] R. Gauld,[55] L. Gavardi,[9] G. Gazzoni,[5] A. Geraci,[21,l] D. Gerick,[11] E. Gersabeck,[11] M. Gersabeck,[54] T. Gershon,[48] Ph. Ghez,[4] A. Gianelle,[22] S. Gianì,[39] V. Gibson,[47] L. Giubega,[29] V. V. Gligorov,[38] C. Göbel,[60] D. Golubkov,[31] A. Golutvin,[53,31,38] A. Gomes,[1,m] C. Gotti,[20,e] M. Grabalosa Gándara,[5] R. Graciani Diaz,[36] L. A. Granado Cardoso,[38] E. Graugés,[36] E. Graverini,[40] G. Graziani,[17] A. Grecu,[29] E. Greening,[55] S. Gregson,[47] P. Griffith,[45] L. Grillo,[11] O. Grünberg,[63] B. Gui,[59] E. Gushchin,[33] Yu. Guz,[35,38] T. Gys,[38] C. Hadjivasiliou,[59] G. Haefeli,[39] C. Haen,[38] S. C. Haines,[47] S. Hall,[53] B. Hamilton,[58] T. Hampson,[46] X. Han,[11] S. Hansmann-Menzemer,[11] N. Harnew,[55] S. T. Harnew,[46] J. Harrison,[54] J. He,[38] T. Head,[39] V. Heijne,[41] K. Hennessy,[52] P. Henrard,[5] L. Henry,[8] J. A. Hernando Morata,[37] E. van Herwijnen,[38] M. Heß,[63] A. Hicheur,[2] D. Hill,[55] M. Hoballah,[5] C. Hombach,[54] W. Hulsbergen,[41] T. Humair,[53] N. Hussain,[55] D. Hutchcroft,[52] D. Hynds,[51] M. Idzik,[27] P. Ilten,[56] R. Jacobsson,[38] A. Jaeger,[11] J. Jalocha,[55] E. Jans,[41] A. Jawahery,[58] F. Jing,[3] M. John,[55] D. Johnson,[38] C. R. Jones,[47] C. Joram,[38] B. Jost,[38] N. Jurik,[59] S. Kandybei,[43] W. Kanso,[6] M. Karacson,[38] T. M. Karbach,[38] S. Karodia,[51] M. Kelsey,[59] I. R. Kenyon,[45] M. Kenzie,[38]

T. Ketel,[42] B. Khanji,[20,38,e] C. Khurewathanakul,[39] S. Klaver,[54] K. Klimaszewski,[28] O. Kochebina,[7] M. Kolpin,[11] I. Komarov,[39] R. F. Koopman,[42] P. Koppenburg,[41,38] M. Korolev,[32] L. Kravchuk,[33] K. Kreplin,[11] M. Kreps,[48] G. Krocker,[11] P. Krokovny,[34] F. Kruse,[9] W. Kucewicz,[26,n] M. Kucharczyk,[26] V. Kudryavtsev,[34] K. Kurek,[28] T. Kvaratskheliya,[31] V. N. La Thi,[39] D. Lacarrere,[38] G. Lafferty,[54] A. Lai,[15] D. Lambert,[50] R. W. Lambert,[42] G. Lanfranchi,[18] C. Langenbruch,[48] B. Langhans,[38] T. Latham,[48] C. Lazzeroni,[45] R. Le Gac,[6] J. van Leerdam,[41] J.-P. Lees,[4] R. Lefèvre,[5] A. Leflat,[32] J. Lefrançois,[7] O. Leroy,[6] T. Lesiak,[26] B. Leverington,[11] Y. Li,[7] T. Likhomanenko,[65,64] M. Liles,[52] R. Lindner,[38] C. Linn,[38] F. Lionetto,[40] B. Liu,[15] S. Lohn,[38] I. Longstaff,[51] J. H. Lopes,[2] P. Lowdon,[40] D. Lucchesi,[22,o] H. Luo,[50] A. Lupato,[22] E. Luppi,[16,b] O. Lupton,[55] F. Machefert,[7] F. Maciuc,[29] O. Maev,[30] K. Maguire,[54] S. Malde,[55] A. Malinin,[64] G. Manca,[15,k] G. Mancinelli,[6] P. Manning,[59] A. Mapelli,[38] J. Maratas,[5] J. F. Marchand,[4] U. Marconi,[14] C. Marin Benito,[36] P. Marino,[23,38,j] R. Märki,[39] J. Marks,[11] G. Martellotti,[25] M. Martinelli,[39] D. Martinez Santos,[42] F. Martinez Vidal,[66] D. Martins Tostes,[2] A. Massafferri,[1] R. Matev,[38] A. Mathad,[48] Z. Mathe,[38] C. Matteuzzi,[20] A. Mauri,[40] B. Maurin,[39] A. Mazurov,[45] M. McCann,[53] J. McCarthy,[45] A. McNab,[54] R. McNulty,[12] B. Meadows,[57] F. Meier,[9] M. Meissner,[11] M. Merk,[41] D. A. Milanes,[62] M.-N. Minard,[4] D. S. Mitzel,[11] J. Molina Rodriguez,[60] S. Monteil,[5] M. Morandin,[22] P. Morawski,[27] A. Mordà,[6] M. J. Morello,[23,j] J. Moron,[27] A. B. Morris,[50] R. Mountain,[59] F. Muheim,[50] J. Müller,[9] K. Müller,[40] V. Müller,[9] M. Mussini,[14] B. Muster,[39] P. Naik,[46] T. Nakada,[39] R. Nandakumar,[49] I. Nasteva,[2] M. Needham,[50] N. Neri,[21] S. Neubert,[11] N. Neufeld,[38] M. Neuner,[11] A. D. Nguyen,[39] T. D. Nguyen,[39] C. Nguyen-Mau,[39,p] V. Niess,[5] R. Niet,[9] N. Nikitin,[32] T. Nikodem,[11] D. Ninci,[23] A. Novoselov,[35] D. P. O'Hanlon,[48] A. Oblakowska-Mucha,[27] V. Obraztsov,[35] S. Ogilvy,[51] O. Okhrimenko,[44] R. Oldeman,[15,k] C. J. G. Onderwater,[67] B. Osorio Rodrigues,[1] J. M. Otalora Goicochea,[2] A. Otto,[38] P. Owen,[53] A. Oyanguren,[66] A. Palano,[13,q] F. Palombo,[21,r] M. Palutan,[18] J. Panman,[38] A. Papanestis,[49] M. Pappagallo,[51] L. L. Pappalardo,[16,b] C. Parkes,[54] G. Passaleva,[17] G. D. Patel,[52] M. Patel,[53] C. Patrignani,[19,i] A. Pearce,[54,49] A. Pellegrino,[41] G. Penso,[25,s] M. Pepe Altarelli,[38] S. Perazzini,[14,g] P. Perret,[5] L. Pescatore,[45] K. Petridis,[46] A. Petrolini,[19,i] M. Petruzzo,[21] E. Picatoste Olloqui,[36] B. Pietrzyk,[4] T. Pilař,[48] D. Pinci,[25] A. Pistone,[19] S. Playfer,[50] M. Plo Casasus,[37] T. Poikela,[38] F. Polci,[8] A. Poluektov,[48,34] I. Polyakov,[31] E. Polycarpo,[2] A. Popov,[35] D. Popov,[10] B. Popovici,[29] C. Potterat,[2] E. Price,[46] J. D. Price,[52] J. Prisciandaro,[39] A. Pritchard,[52] C. Prouve,[46] V. Pugatch,[44] A. Puig Navarro,[39] G. Punzi,[23,t] W. Qian,[4] R. Quagliani,[7,46] B. Rachwal,[26] J. H. Rademacker,[46] B. Rakotomiaramanana,[39] M. Rama,[23] M. S. Rangel,[2] I. Raniuk,[43] N. Rauschmayr,[38] G. Raven,[42] F. Redi,[53] S. Reichert,[54] M. M. Reid,[48] A. C. dos Reis,[1] S. Ricciardi,[49] S. Richards,[46] M. Rihl,[38] K. Rinnert,[52] V. Rives Molina,[36] P. Robbe,[7,38] A. B. Rodrigues,[1] E. Rodrigues,[54] J. A. Rodriguez Lopez,[62] P. Rodriguez Perez,[54] S. Roiser,[38] V. Romanovsky,[35] A. Romero Vidal,[37] M. Rotondo,[22] J. Rouvinet,[39] T. Ruf,[38] H. Ruiz,[36] P. Ruiz Valls,[66] J. J. Saborido Silva,[37] N. Sagidova,[30] P. Sail,[51] B. Saitta,[15,k] V. Salustino Guimaraes,[2] C. Sanchez Mayordomo,[66] B. Sanmartin Sedes,[37] R. Santacesaria,[25] C. Santamarina Rios,[37] M. Santimaria,[18] E. Santovetti,[24,h] A. Sarti,[18,s] C. Satriano,[25,c] A. Satta,[24] D. M. Saunders,[46] D. Savrina,[31,32] M. Schiller,[38] H. Schindler,[38] M. Schlupp,[9] M. Schmelling,[10] T. Schmelzer,[9] B. Schmidt,[38] O. Schneider,[39] A. Schopper,[38] M.-H. Schune,[7] R. Schwemmer,[38] B. Sciascia,[18] A. Sciubba,[25,s] A. Semennikov,[31] I. Sepp,[53] N. Serra,[40] J. Serrano,[6] L. Sestini,[22] P. Seyfert,[11] M. Shapkin,[35] I. Shapoval,[16,43,b] Y. Shcheglov,[30] T. Shears,[52] L. Shekhtman,[34] V. Shevchenko,[64] A. Shires,[9] R. Silva Coutinho,[48] G. Simi,[22] M. Sirendi,[47] N. Skidmore,[46] I. Skillicorn,[51] T. Skwarnicki,[59] E. Smith,[55,49] E. Smith,[53] J. Smith,[47] M. Smith,[54] H. Snoek,[41] M. D. Sokoloff,[57,38] F. J. P. Soler,[51] F. Soomro,[39] D. Souza,[46] B. Souza De Paula,[2] B. Spaan,[9] P. Spradlin,[51] S. Sridharan,[38] F. Stagni,[38] M. Stahl,[11] S. Stahl,[38] O. Steinkamp,[40] O. Stenyakin,[35] F. Sterpka,[59] S. Stevenson,[55] S. Stoica,[29] S. Stone,[59] B. Storaci,[40] S. Stracka,[23,j] M. Straticiuc,[29] U. Straumann,[40] R. Stroili,[22] L. Sun,[57] W. Sutcliffe,[53] K. Swientek,[27] S. Swientek,[9] V. Syropoulos,[42] M. Szczekowski,[28] P. Szczypka,[39,38] T. Szumlak,[27] S. T'Jampens,[4] T. Tekampe,[9] M. Teklishyn,[7] G. Tellarini,[16,b] F. Teubert,[38] C. Thomas,[55] E. Thomas,[38] J. van Tilburg,[41] V. Tisserand,[4] M. Tobin,[39] J. Todd,[57] S. Tolk,[42] L. Tomassetti,[16,b] D. Tonelli,[38] S. Topp-Joergensen,[55] N. Torr,[55] E. Tournefier,[4] S. Tourneur,[39] K. Trabelsi,[39] M. T. Tran,[39] M. Tresch,[40] A. Trisovic,[38] A. Tsaregorodtsev,[6] P. Tsopelas,[41] N. Tuning,[41,38] A. Ukleja,[28] A. Ustyuzhanin,[65,64] U. Uwer,[11] C. Vacca,[15,k] V. Vagnoni,[14] G. Valenti,[14] A. Vallier,[7] R. Vazquez Gomez,[18] P. Vazquez Regueiro,[37] C. Vázquez Sierra,[37] S. Vecchi,[16] J. J. Velthuis,[46] M. Veltri,[17,u] G. Veneziano,[39] M. Vesterinen,[11] B. Viaud,[7] D. Vieira,[2] M. Vieites Diaz,[37] X. Vilasis-Cardona,[36,f] A. Vollhardt,[40] D. Volyanskyy,[10] D. Voong,[46] A. Vorobyev,[30] V. Vorobyev,[34] C. Voß,[63] J. A. de Vries,[41] R. Waldi,[63] C. Wallace,[48] R. Wallace,[12] J. Walsh,[23] S. Wandernoth,[11] J. Wang,[59] D. R. Ward,[47] N. K. Watson,[45] D. Websdale,[53] A. Weiden,[40] M. Whitehead,[48] D. Wiedner,[11] G. Wilkinson,[55,38] M. Wilkinson,[59] M. Williams,[38] M. P. Williams,[45] M. Williams,[56] F. F. Wilson,[49] J. Wimberley,[58] J. Wishahi,[9] W. Wislicki,[28] M. Witek,[26] G. Wormser,[7] S. A. Wotton,[47] S. Wright,[47] K. Wyllie,[38] Y. Xie,[61] Z. Xu,[39] Z. Yang,[3]

X. Yuan,[34] O. Yushchenko,[35] M. Zangoli,[14] M. Zavertyaev,[10,v] L. Zhang,[3] Y. Zhang,[3] A. Zhelezov,[11] A. Zhokhov,[31] and L. Zhong[3]

(LHCb Collaboration)

[1]*Centro Brasileiro de Pesquisas Físicas (CBPF), Rio de Janeiro, Brazil*
[2]*Universidade Federal do Rio de Janeiro (UFRJ), Rio de Janeiro, Brazil*
[3]*Center for High Energy Physics, Tsinghua University, Beijing, China*
[4]*LAPP, Université Savoie Mont-Blanc, CNRS/IN2P3, Annecy-Le-Vieux, France*
[5]*Clermont Université, Université Blaise Pascal, CNRS/IN2P3, LPC, Clermont-Ferrand, France*
[6]*CPPM, Aix-Marseille Université, CNRS/IN2P3, Marseille, France*
[7]*LAL, Université Paris-Sud, CNRS/IN2P3, Orsay, France*
[8]*LPNHE, Université Pierre et Marie Curie, Université Paris Diderot, CNRS/IN2P3, Paris, France*
[9]*Fakultät Physik, Technische Universität Dortmund, Dortmund, Germany*
[10]*Max-Planck-Institut für Kernphysik (MPIK), Heidelberg, Germany*
[11]*Physikalisches Institut, Ruprecht-Karls-Universität Heidelberg, Heidelberg, Germany*
[12]*School of Physics, University College Dublin, Dublin, Ireland*
[13]*Sezione INFN di Bari, Bari, Italy*
[14]*Sezione INFN di Bologna, Bologna, Italy*
[15]*Sezione INFN di Cagliari, Cagliari, Italy*
[16]*Sezione INFN di Ferrara, Ferrara, Italy*
[17]*Sezione INFN di Firenze, Firenze, Italy*
[18]*Laboratori Nazionali dell'INFN di Frascati, Frascati, Italy*
[19]*Sezione INFN di Genova, Genova, Italy*
[20]*Sezione INFN di Milano Bicocca, Milano, Italy*
[21]*Sezione INFN di Milano, Milano, Italy*
[22]*Sezione INFN di Padova, Padova, Italy*
[23]*Sezione INFN di Pisa, Pisa, Italy*
[24]*Sezione INFN di Roma Tor Vergata, Roma, Italy*
[25]*Sezione INFN di Roma La Sapienza, Roma, Italy*
[26]*Henryk Niewodniczanski Institute of Nuclear Physics Polish Academy of Sciences, Kraków, Poland*
[27]*AGH - University of Science and Technology, Faculty of Physics and Applied Computer Science, Kraków, Poland*
[28]*National Center for Nuclear Research (NCBJ), Warsaw, Poland*
[29]*Horia Hulubei National Institute of Physics and Nuclear Engineering, Bucharest-Magurele, Romania*
[30]*Petersburg Nuclear Physics Institute (PNPI), Gatchina, Russia*
[31]*Institute of Theoretical and Experimental Physics (ITEP), Moscow, Russia*
[32]*Institute of Nuclear Physics, Moscow State University (SINP MSU), Moscow, Russia*
[33]*Institute for Nuclear Research of the Russian Academy of Sciences (INR RAN), Moscow, Russia*
[34]*Budker Institute of Nuclear Physics (SB RAS) and Novosibirsk State University, Novosibirsk, Russia*
[35]*Institute for High Energy Physics (IHEP), Protvino, Russia*
[36]*Universitat de Barcelona, Barcelona, Spain*
[37]*Universidad de Santiago de Compostela, Santiago de Compostela, Spain*
[38]*European Organization for Nuclear Research (CERN), Geneva, Switzerland*
[39]*Ecole Polytechnique Fédérale de Lausanne (EPFL), Lausanne, Switzerland*
[40]*Physik-Institut, Universität Zürich, Zürich, Switzerland*
[41]*Nikhef National Institute for Subatomic Physics, Amsterdam, The Netherlands*
[42]*Nikhef National Institute for Subatomic Physics and VU University Amsterdam, Amsterdam, The Netherlands*
[43]*NSC Kharkiv Institute of Physics and Technology (NSC KIPT), Kharkiv, Ukraine*
[44]*Institute for Nuclear Research of the National Academy of Sciences (KINR), Kyiv, Ukraine*
[45]*University of Birmingham, Birmingham, United Kingdom*
[46]*H.H. Wills Physics Laboratory, University of Bristol, Bristol, United Kingdom*
[47]*Cavendish Laboratory, University of Cambridge, Cambridge, United Kingdom*
[48]*Department of Physics, University of Warwick, Coventry, United Kingdom*
[49]*STFC Rutherford Appleton Laboratory, Didcot, United Kingdom*
[50]*School of Physics and Astronomy, University of Edinburgh, Edinburgh, United Kingdom*
[51]*School of Physics and Astronomy, University of Glasgow, Glasgow, United Kingdom*
[52]*Oliver Lodge Laboratory, University of Liverpool, Liverpool, United Kingdom*

[53]*Imperial College London, London, United Kingdom*
[54]*School of Physics and Astronomy, University of Manchester, Manchester, United Kingdom*
[55]*Department of Physics, University of Oxford, Oxford, United Kingdom*
[56]*Massachusetts Institute of Technology, Cambridge, MA, United States*
[57]*University of Cincinnati, Cincinnati, OH, United States*
[58]*University of Maryland, College Park, MD, United States*
[59]*Syracuse University, Syracuse, NY, United States*
[60]*Pontifícia Universidade Católica do Rio de Janeiro (PUC-Rio), Rio de Janeiro, Brazil (associated with Institution Universidade Federal do Rio de Janeiro (UFRJ), Rio de Janeiro, Brazil)*
[61]*Institute of Particle Physics, Central China Normal University, Wuhan, Hubei, China (associated with Institution Center for High Energy Physics, Tsinghua University, Beijing, China)*
[62]*Departamento de Fisica, Universidad Nacional de Colombia, Bogota, Colombia (associated with LPNHE, Université Pierre et Marie Curie, Université Paris Diderot, CNRS/IN2P3, Paris, France)*
[63]*Institut für Physik, Universität Rostock, Rostock, Germany (associated with Institution Physikalisches Institut, Ruprecht-Karls-Universität Heidelberg, Heidelberg, Germany)*
[64]*National Research Centre Kurchatov Institute, Moscow, Russia (associated with Institution Institute of Theoretical and Experimental Physics (ITEP), Moscow, Russia)*
[65]*Yandex School of Data Analysis, Moscow, Russia (associated with Institution Institute of Theoretical and Experimental Physics (ITEP), Moscow, Russia)*
[66]*Instituto de Fisica Corpuscular (IFIC), Universitat de Valencia-CSIC, Valencia, Spain (associated with Institution Universitat de Barcelona, Barcelona, Spain)*
[67]*Van Swinderen Institute, University of Groningen, Groningen, The Netherlands (associated with Institution Nikhef National Institute for Subatomic Physics, Amsterdam, The Netherlands)*

[a]Also at Università di Firenze, Firenze, Italy.
[b]Also at Università di Ferrara, Ferrara, Italy.
[c]Also at Università della Basilicata, Potenza, Italy.
[d]Also at Università di Modena e Reggio Emilia, Modena, Italy.
[e]Also at Università di Milano Bicocca, Milano, Italy.
[f]Also at LIFAELS, La Salle, Universitat Ramon Llull, Barcelona, Spain.
[g]Also at Università di Bologna, Bologna, Italy.
[h]Also at Università di Roma Tor Vergata, Roma, Italy.
[i]Also at Università di Genova, Genova, Italy.
[j]Also at Scuola Normale Superiore, Pisa, Italy.
[k]Also at Università di Cagliari, Cagliari, Italy.
[l]Also at Politecnico di Milano, Milano, Italy.
[m]Also at Universidade Federal do Triângulo Mineiro (UFTM), Uberaba-MG, Brazil.
[n]Also at AGH—University of Science and Technology, Faculty of Computer Science, Electronics and Telecommunications, Kraków, Poland.
[o]Also at Università di Padova, Padova, Italy.
[p]Also at Hanoi University of Science, Hanoi, Viet Nam.
[q]Also at Università di Bari, Bari, Italy.
[r]Also at Università degli Studi di Milano, Milano, Italy.
[s]Also at Università di Roma La Sapienza, Roma, Italy.
[t]Also at Università di Pisa, Pisa, Italy.
[u]Also at Università di Urbino, Urbino, Italy.
[v]Also at P.N. Lebedev Physical Institute, Russian Academy of Science (LPI RAS), Moscow, Russia.